A NOVEL METHOD FOR CALIBRATION OF AEROSOL DATABASES WITH LIDAR-CEILOMETER MEASUREMENTS

D. Bachour, D. Perez-Astudillo, L. Martin-Pomares

Qatar Environment & Energy Research Institute, Qatar Foundation, HBKU, Doha, Qatar

Abstract

Satellite observations and chemical transport models used for the derivation of Aerosol Optical Depth (AOD) values have an extensive coverage worldwide and are widely used when ground-measured AOD is not available. However, satellite and modelled values present high uncertainties and cannot be always considered reliable especially at the level needed for solar radiation modelling. This work presents a methodology for calibrating existing AOD databases, which are commonly used as inputs to clear sky models for estimating clear-sky solar irradiances. This methodology makes use of ground-measured direct normal irradiance (*Hb*), integrated backscatter profiles of a lidar-ceilometer device, and *Hb* calculated from clear sky models with different AOD databases.

Keywords: *AOD, lidar, ceilometer, aerosol loads, DNI*

1. Introduction

In clear skies, aerosols are the main atmospheric component absorbing and scattering solar radiation. Their atmospheric extinction is generally described in terms of Aerosol Optical Depth (AOD), a useful parameter for the calculation of clear-sky solar irradiances. AOD can be directly measured by ground-based sun-photometers [Holben et al, 1998], or derived from satellite images such as MISR [Keller et al, 2007] and MODIS [Kosmopoulos et al, 2008] and from chemical transport models such as MACC [Cebecauer and Suri, 2010]. The direct measurements are the best option for determining AOD, but they have limited coverage. The indirect sources have wider coverage, but provide AOD data with lower temporal and spatial resolutions, and exhibit high uncertainties particularly in regions of high aerosol loads [Cebecauer et al, 2011; Gueymard, 2012].

Lidar-ceilometers measure atmospheric backscatter profiles as a function of time and height in the atmosphere. These profiles are normally used for the determination of the boundary layer height and cloud base height [Munkel, 2006]. However, they can also be used to extract aerosol information that can be used as an alternative to the AOD parameter in the modelling of solar radiation; indeed, a good correlation was found between lidar-ceilometer measurements and direct normal irradiance ground measurements in [Bachour and Perez-Astudillo, 2014].

2. Instrumentation and data used

The experimental data used here consist of clear days in the time interval 10 am to 1 pm, collected over a period of 12 months from December 2012 to November 2013. 214 clear days were selected for the analysis presented in this paper. The Vaisala ceilometer CL51 was used for the recording of the range-corrected atmospheric backscatter profiles. It uses a 910 nm pulsed diode laser. The reported backscattered signal has a vertical resolution of 10 m, with 15 km as maximum range. For more details about the CL51 instrument, the reader can refer to [Vaisala, 2015]. A CHP1 pyrheliometer [CHP1, 2015] mounted on a high precision Kipp and Zonen solar radiation monitoring station was used for the measurements of the direct normal irradiance as one-minute averages in W/m^2.

The clear-sky irradiation values used here were derived from the McClear and REST2 models. McClear estimates the solar radiation at ground level under clear sky conditions by using the abaci approach and interpolation functions. It uses mainly inputs from the MACC project. Aerosol information used by the McClear model consists of aerosol optical depth at 550 nm, Angström coefficient, and aerosol type from the MACC database. The model has been validated at several BSRN stations and gives good results [Lefèvre, 2013]. REST2 is a high-performance radiative model used to predict clear-sky broadband irradiances. It uses the Angström turbidity coefficient, the Angström wavelength exponent and aerosol single-scattering albedo as aerosol inputs to the model [Gueymard, 2008]. It is possible to use any AOD data with this model. For the irradiation data presented here, the aerosol information used with the REST2 model is extracted from the MISR and MACC databases.

doi:10.18086/swc.2015.07.19 Available at http://proceedings.ises.org

3. Methodology

The backscattered intensity profiles recorded by the CL51 during a clear day depend on the aerosol constituents of the atmosphere and provide information on their height as a function of time. Of interest for this analysis, are the atmospheric backscatter coefficients recorded as a two-dimensional dataset values, reported every 36 s, in 10-m steps up to 15 km height. From these measured backscatter coefficients, the hourly-averaged backscatter coefficients were obtained for each height step and summed thereafter up to 5 km height in the atmosphere. The 5 km height limit in the atmosphere was found to be representative of the dynamicity of the atmosphere in the studied location. The obtained integrated backscatter coefficient, named hereby the beta coefficient, is the starting point of the calibration method using lidar-ceilometer measurements as suggested here.

This high-resolution local aerosol information is used to validate indirectly the aerosol databases by measuring the performance of a clear-sky model through the hereby-called 'performance ratio':

$$Kp\_cs = Hb\_cs / Hb\_m, \qquad \text{(eq. 1)}$$

Where *Hb_m* is the ground-measured value of the hourly beam irradiance (also called DNI, direct normal irradiance) obtained from the quality-controlled 1-minute values of measured direct normal irradiance. The applied quality control checks follow the BSRN standards [Long and Dutton, 2002]. *Hb_cs* is the corresponding modelled clear-sky value, derived from a clear-sky model. This ratio measures the performance of the used clear-sky model. The calculated performance is then correlated to the corresponding measured integrated backscatter, the beta coefficient, and the resulting correlation is used in order to correct the DNI values derived from the clear-sky model. This way, aerosol information used as input to the clear-sky model is indirectly calibrated.

4. Results and discussion

Fig.1 shows the ratio of the DNI derived from the clear sky model McClear versus the ground-measured DNI, as a function of the integrated backscatter lidar-ceilometer signal. Fig.2 and Fig.3 show the performance ratio of the REST2 model using aerosol information from MISR and from MACC, respectively, as a function of the integrated backscatter lidar-ceilometer sigmal.

It can be seen that up to a certain value of the beta coefficient, the clear-sky models performs reasonably well; for higher values of the integrated backscatter coefficient, i.e., high aerosol loads, the performance of the clear-sky models degrades and leads to an overestimation of the direct normal irradiance, most likely related to an underestimation of aerosols in the used databases, as has been also shown by [Jiang et al, 2007] and [Polo and Estalayo, 2015].

The overestimation in DNI can be correlated with the integrated backscatter measurements derived from the lidar-ceilometer. The correlation will be used to calibrate the clear-sky models for high aerosol loads.

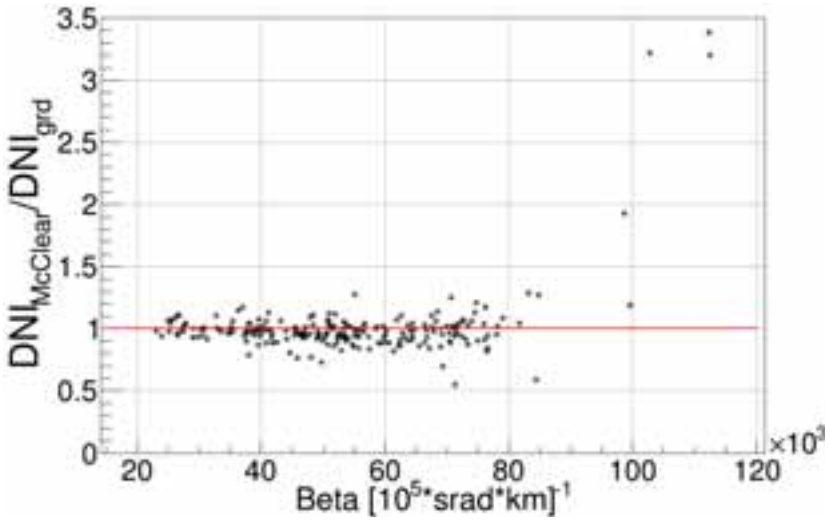

Fig. 1: Performance of the McClear model-derived beam irradiance vs. the integrated backscatter coefficient, at the hour from 11 am to 12 pm.

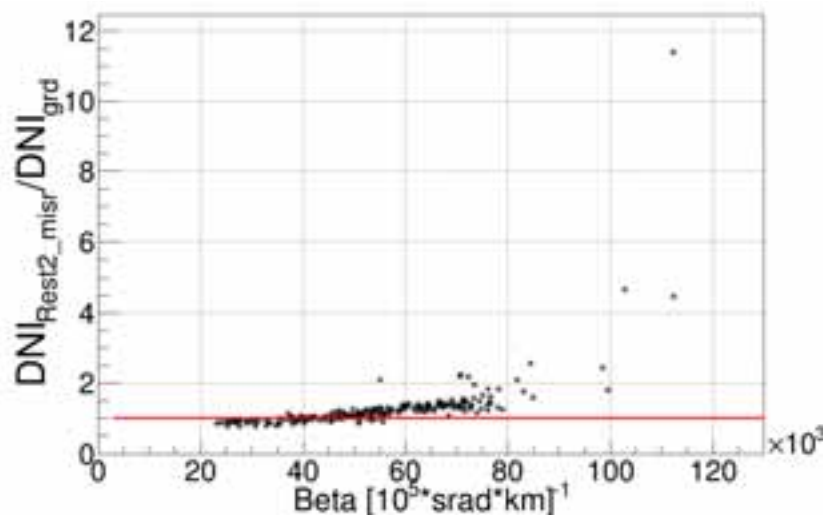

Fig. 2: Performance of the REST2 model-derived beam irradiance using aerosol from MISR vs. the integrated backscatter coefficient, at the hour from 11 am to 12 pm.

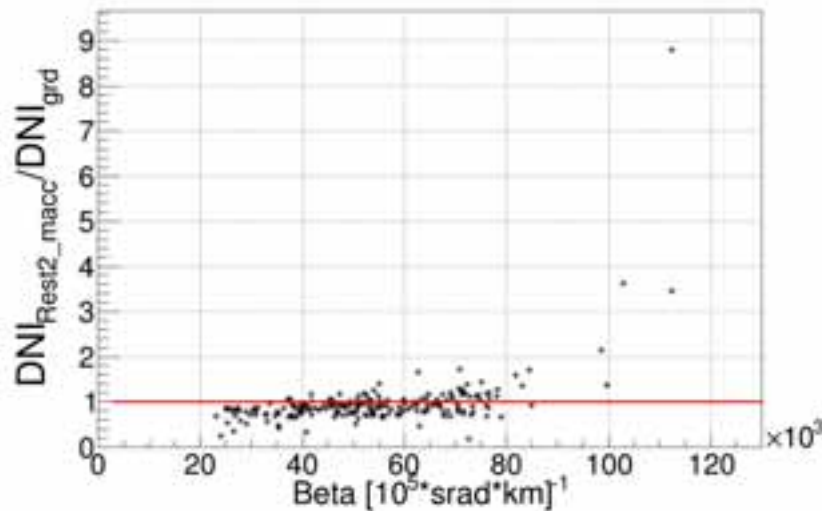

Fig. 3: Performance of the REST2 model-derived beam irradiance using aerosol from MACC vs. the integrated backscatter coefficient, at the hour from 11 am to 12 pm.

The decrease in performance at high beta values was quantified using an exponential function fitted to the ratios corresponding to beta values around 70000×10^5 $[srad.km]^{-1}$ and higher, where poor performance of the clear-sky models can be seen. The equation of the fit is the following:

$$Hb\_cs / Hb\_m = CF = \exp(slope * Beta + const), \quad \text{(eq. 2)}$$

Where Beta is the sum up to 5 km of the hourly-averaged backscatter lidar signals, *Hb_cs* is the hourly DNI derived from the clear-sky model, *Hb_m* is the hourly DNI derived from the ground measurements. *CF* stands for calibration function, and *slope* and *const* are parameters obtained from the applied fit.

The fitted function can then be used to correct the DNI values derived from the clear sky models for Beta values higher than the used Beta limit. The correction can be written as follows:

$$Hb\_cs,corr = Hb\_cs / CF, \quad \text{(eq. 3)}$$

where *Hb_cs,corr* is the corrected value of *Hb_cs*.

By using Eq.3 to calibrate the clear-sky model, the aerosol information used as input to the model is indirectly calibrated as a function of the lidar-ceilometer measurements.

Fig. 4 shows the performance of the corrected McClear model, after applying the function in Eq.3. The effectiveness of the calibration method as applied to the McClear model is noticeable on the data points corresponding to high beta values, i.e., high aerosol loads. The calibration of the REST2 model using MISR and MACC databases (not shown here) confirms the same.

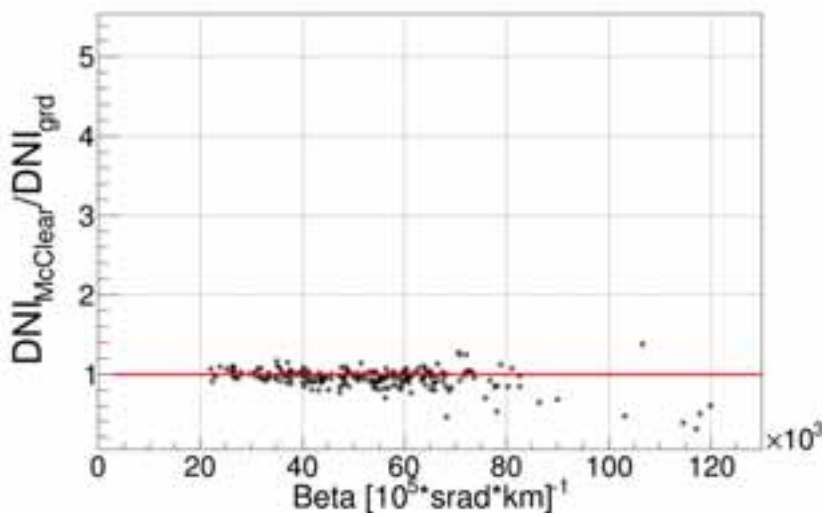

Fig. 4: Performance after calibration of the McClear model-derived beam irradiance vs. the integrated backscatter coefficient, at the hour from 11 am to 12 pm.

The effect of the suggested method on the calibration of the McClear model was evaluated using the relative mean bias error (MBE) and root-mean-square error (RMSE) of the performance ratios before and after calibration for different periods of time. The results for the hour 11 and 13 are listed in Table 1 and Table 2, respectively.

Tab. 1: Statistical indicators of the comparison of clear-sky model against clear-sky calibrated model using the beta coefficient, for the hour 10 to 11. rMBE and rRMSE are in %.

Model	rMBE	rRMSE
BEFORE CALIBRATION		
McClear	-1.05	24.16
REST2 with MISR	24.71	93.51
REST2 with MACC	-6.86	69.41
AFTER CALIBRATION		
McClear	-5.11	14.2
REST2 with MISR	8.36	25.16
REST2 with MACC	-14.64	29.67

Tab. 2: Statistical indicators of the comparison of clear-sky model against clear-sky calibrated model using the beta coefficient, for the hour 12 to 13. rMBE and rRMSE are in %.

Model	rMBE	rRMSE
BEFORE CALIBRATION		
McClear	1.96	29.22
REST2 with MISR	31.48	107.33
REST2 with MACC	-0.25	79.63
AFTER CALIBRATION		
McClear	-5.09	15.53
REST2 with MISR	5.5	23.98
REST2 with MACC	-13.18	27.37

Table 1 and Table 2 show that the calibrated dataset has lower rRMSE values for all the clear sky models as compared to the original clear-sky datasets. The rMBE value for the calibrated REST2 model with MISR database is also lower than the relative bias of the uncalibrated model, but higher for the calibrated clear-sky models using the MACC database. Since the calibration was only applied to the points with high beta values, the rMBE of the calibrated models shown in the tables are now dominated by the bias of the points with lower beta values; this discrepancy can be easily reduced and will provide smaller relative bias values when calibrating the DNI using all Beta values in the fit to obtain *CF*.

The noticeable decrease in the relative errors, when comparing the results before and after applying the suggested calibration method on the clear-sky models, shows the effectiveness of using the lidar ceilometer measurements as local aerosol information, which can be ultimately used as a reliable tool to correct the existing aerosol databases.

5. References

Bachour, D., Perez-Astudillo, D., 2014. Deriving solar direct normal irradiance using lidar-ceilometer. Solar Energy. 110, 316-324.

Cebecauer, T., Suri, M., 2010. Accuracy improvements of satellite-derived solar resource based on GEMS re-analysis aerosols. Proceedings of SolarPACES International Conference.

Cebecauer, T., Suri, M., Gueymard, C.A., 2011. Uncertainty sources in satellite-derived direct normal irradiance: how can prediction accuracy be improved globally?. Proceedings of SolarPACES International Conference.

Gueymard, C.A., 2008. REST2: High-performance solar radiation model for cloudless-sky irradiance, illuminance, and photosynthetically active radiation – Validation with a benchmark dataset. Solar Energy. 82(3), 272-285.

Gueymard, C.A., 2012. Temporal variability in direct and global irradiance at various time scales as affected by aerosols. Solar Energy 86, 3544–3553.

Holben, B.N., Eck, T.F., Slutsker, I., Tanre, D., Buis, J.P., Setzer, A., Vermote, E., Reagan, J.A., Kaufman, Y.J., Nakajima, T., Lavenu, F., Jankowiak, I., Smirnov, A., 1998. AERONET - A federated instrument network and data archive for aerosol characterization. Remote Sensing of Environment. 66(1):1-16.

Jiang, X., Liu, Y., Yu, B., Jiang, M., 2007. Comparison of MISR aerosol optical thickness with AERONET measurements in Beijing metropolitan area. Remote sensing of environment. 107 (1-2), 45-53.

Keller, J., Bojinski, S., Prevot, S.H., 2007. Simultaneous retrieval of aerosol and surface optical properties using data of the Multi-angle Imaging SpectroRadiometer (MISR). Remote Sensing of Environment. 107(1-2),120-137.

Kosmopoulos, P.G., Kaskaoutis, D.G., Nastos, P.T., Kambezidis, H.D., 2008. Seasonal variation of columnar aerosol optical properties over Athens, Greece, based on MODIS data. Remote Sensing of Environment.112(5), 2354-2366.

Lefèvre, M., Oumbe, A., Blanc, P., Espinar, B., Gschwind, B., Qu, Z., Wald, L.,Schroedter-Homscheidt, M., Hoyer-Klick, C., Arola, A., Benedetti, A., Kaiser, J.W.,Morcrette, J.J., 2013. McClear: a new model estimating downwelling solar radiation at ground level in clear-sky conditions. Atmospheric Measurement Techniques. 6, 2403-2418.

Long, C.N., Dutton. E.G., 2002. BSRN global network recommended QC tests, v2.0. BSRN Technical Report.

Munkel, C., 2006. Boundary layer and air quality monitoring with a commercial lidar ceilometer. Proc. SPIE 6367.

Polo., J, Estalayo., G, 2015. Impact of atmospheric aerosol loads on Concentrating Solar Power production in arid-desert sites. Solar Energy. 115, 621-631

CHP1, 2015. http://www.kippzonen.com/?downloadcategory/19192/Pyrheliometers.aspx. Last accessed September 2015.

Vaisala, 2015. http://www.vaisala.com/en/products/ceilometers/Pages/cl51.aspx. Last accessed September 2015.